The dynamic range of poleward energy transport in an atmospheric general circulation model

Rodrigo Caballero
Department of the Geophysical Sciences, University of Chicago, Chicago, Illinois, USA

Peter L. Langen
Department of Geophysics, University of Copenhagen, Copenhagen, Denmark

Received 21 September 2004; revised 19 November 2004; accepted 30 December 2004; published 27 January 2005.

[1] Understanding the reasons for which current climate models fail to reproduce the low equator-to-pole temperature gradient of past warm periods is among the major challenges in climate science. We focus here on the role of atmospheric poleward heat transport. We use an aquaplanet general circulation model (GCM) to construct a regime diagram of this quantity as a function of surface temperature and its meridional gradient, encompassing the range experienced by Earth over the Cenozoic. We find that poleward heat transport increases with surface temperature over much of this range, but saturates in the low-gradient, high-temperature regime where it is most needed. We identify some specific dynamical feedbacks responsible for this behavior: increasing tropospheric static stability and poleward migration of the storm tracks as global-mean temperature increases. **Citation:** Caballero, R., and P. L. Langen (2005), The dynamic range of poleward energy transport in an atmospheric general circulation model, *Geophys. Res. Lett.*, *32*, L02705, doi:10.1029/2004GL021581.

1. Introduction

[2] An outstanding problem in climate science is to reconcile the geological proxy record for past warm climates, which indicates elevated global-mean surface temperatures and weak equator-to-pole temperature gradients [*Greenwood and Wing*, 1995; *Crowley and Zachos*, 2000], with numerical simulations of those periods, which easily reproduce the proxy-inferred global-mean temperatures given a plausible increase in greenhouse gas concentrations, but fall far short of attaining the observed reduction in meridional gradient [*Barron*, 1987; *Huber and Sloan*, 2001]. Some authors [*Schmidt and Mysak*, 1996; *Hay et al.*, 1997] have suggested that atmospheric heat transport may play an important role in resolving this "low gradient paradox". It is plausible to expect a warmer atmosphere to transport more latent heat poleward, helping reduce meridional temperature gradients. Moreover, the exponential increase of saturation vapor pressure with temperature suggests that the feedback could become increasingly powerful as temperature rises. The ongoing upward revision of proxy-inferred Cretaceous and Eocene tropical sea surface temperature thus makes this mechanism especially appealing [*Norris et al.*, 2002].

[3] So why does poleward heat transport not play a more salient role in reducing meridional temperature gradients in climate models? Studies of this question have hitherto been somewhat piecemeal, comparing a reference climate with a single or only a few perturbed cases, sometimes confirming [*Manabe and Wetherald*, 1980] and sometimes negating [*Pierrehumbert*, 2002] its relevance. Here, we take a comprehensive approach, presenting a systematic study of poleward energy transport in an atmospheric GCM over a broad range of global mean surface temperatures and meridional gradients. This extends previous work employing fixed surface temperature [e.g., *Rind*, 1998; *Huber and Sloan*, 1999], permitting a more robust identification of underlying physical mechanisms. Our key result is that, though latent heat transport indeed increases with temperature, it does not do so indefinitely. Rather, significant changes take place in the atmospheric general circulation which cause poleward heat flux to saturate at high temperatures.

2. Poleward Energy Transport as a Function of Surface Temperature

[4] We use PCCM3, the atmospheric component of the Fast Ocean-Atmosphere Model (FOAM [*Jacob*, 1997]), which combines the dynamical core of NCAR's CCM2 with the physical parameterizations of CCM3.6 [*Kiehl et al.*, 1996]. We use T42 resolution, sufficient to adequately capture midlatitude storm-track dynamics [*Dong and Valdes*, 2000]. In the interest of simplicity, and since we are focusing here on zonal-mean quantities, we use aquaplanet boundary conditions. The model is run with fixed, zonally symmetric surface temperature $T_s(\varphi) = T_m - \Delta T\ (3\ \sin^2\ \varphi\ -\ 1)/3$, where T_m is the global mean temperature, ΔT is the equator-pole temperature difference and φ is latitude. Sea ice is specified where $T_s < 0°C$. We vary T_m and ΔT at 5°C intervals in the range 0–35°C and 10–60°C, respectively. For each (T_m, ΔT) combination, we run the model for 4 years, taking statistics over the last 3 years. We exclude cases where $T_s > 45°C$ at the equator, as it is doubtful that the model can realistically handle such extreme temperatures.

[5] We compute meridional energy transport indirectly—that is, we assume zero long-term energy storage in each atmospheric column, so that $\nabla \cdot \mathbf{F} = R - S$, where $\mathbf{F}$ is the vertically-integrated, time-mean horizontal atmospheric energy flux, while R and S are time-mean vertical energy fluxes at the top of the model and surface respectively. The total northward atmospheric energy flux across latitude φ is computed by integrating the above expression zonally and meridionally from the south pole to φ. The meridional latent

0094-8276/05/2004GL021581$05.00

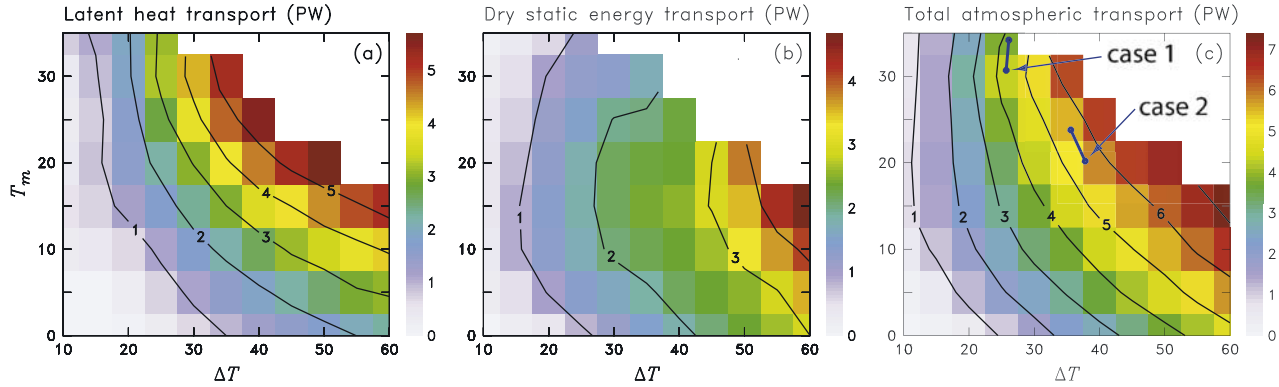

Figure 1. Peak extratropical poleward transport of (a) latent heat, (b) dry static energy and (c) total energy (dry+latent). Blue segments in Figure 1c show T_m and ΔT in the slab ocean runs (see text).

heat flux is similarly computed from the expression $\nabla \cdot \mathbf{F_L} = -L_v\,(P - E)$, where $\mathbf{F_L}$ is the horizontal latent heat flux, L_v is the latent heat of vaporization, P is the precipitation rate and E the surface evaporation rate. The dry static energy flux is taken as the residual of the total and latent heat fluxes.

[6] We focus here on the behavior of energy fluxes in the extratropics, defined as the zone poleward of 25° latitude. In this region, the poleward energy fluxes invariably have a single, well-defined maximum. These peak extratropical energy fluxes are plotted in Figure 1 as a function of T_m and ΔT. It may be argued that atmospheric transports will reduce tropospheric meridional temperature gradients below the value imposed at the surface, so it may be more suitable to plot results as a function of this internal temperature gradient. As it turns out, this reduction is modest and does not affect our qualitative conclusions. We retain ΔT as the independent variable as this is most easily compared with paleoclimate reconstructions.

[7] Figure 1a shows that latent heat transport generally increases with both T_m and ΔT, except in the low-gradient, high-temperature regime where the dependence on T_m becomes very weak. The dry static energy flux increases with ΔT, as we would expect, but there is a strong dependence also on T_m, with a broad maximum centered around T_m = 15–20°C and a decrease at higher temperatures. In the region with $T_m > 15$°C and $\Delta T < 30$°C, the combined behavior of latent and dry static energy transports results in a total transport essentially independent of T_m. In this region, which contains the climates of the Late Cretaceous and Early Paleogene, increasing T_m cannot lead to decreased ΔT through greater heat transport.

3. Mechanisms Limiting Poleward Energy Transport at High Temperatures

[8] Poleward latent heat transport

$$F_L(\varphi) = \frac{L_v}{g} a \cos\varphi \iint v q \, d\lambda \, dp, \tag{1}$$

where v is northward velocity, q specific humidity, λ is longitude and p is pressure, is dominated in the extratropics by eddy fluxes in the storm tracks. The eddies pick up moisture at low levels on the equatorward flank of the storm track and transport it poleward and upward, where lower temperatures cause condensation and latent heat release. This picture suggests the following plausible scaling for F_L:

$$V q_s(T_{\mathrm{src}}), \tag{2}$$

where V is a typical meridional velocity scale, q_s is saturation specific humidity and T_{src} is a near-surface

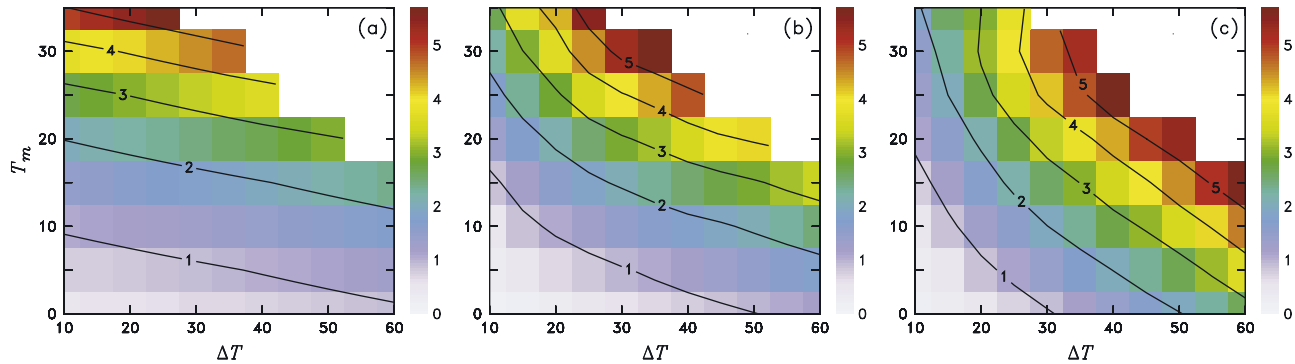

Figure 2. Poleward latent heat transport estimated (a) as $AV\,q_s(T_{\mathrm{src}})$ with $V = 10$ m s^{-1}, $T_{\mathrm{src}} = T_s(25°)$, and A an arbitrary constant; (b) as in (a), but with V taken from the model (Figure 3a); (c) as $A \cos\varphi_{st}\, V\, q_s(T_{\mathrm{src}})$, where V is taken from the model, φ_{st} is the latitude of the model storm track axis (Figure 3b), $T_{\mathrm{src}} = T_s(\varphi_H)$ and φ_H is the poleward boundary of the Hadley cell.

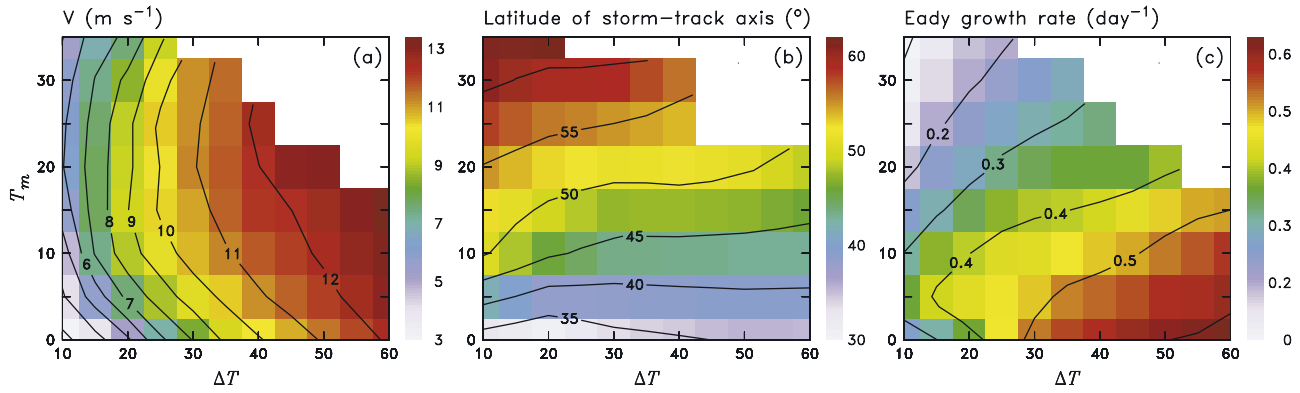

Figure 3. (a) Velocity scale V estimated from the model runs as $\sqrt{2\,EKE}$, where EKE is eddy kinetic energy averaged over a 30° latitude band around the storm-track axis below 500 hPa. (b) Latitude of the storm-track axis, defined as the location of maximum EKE below 500 hPa. (c) Eady growth rate σ_{BI} averaged over the same region as in Figure 3a.

temperature representative of the subtropical moisture source regions [*Pierrehumbert*, 2002]. If neither V nor the location of the source regions change, the flux will increase exponentially with $T_{\rm src}$ and thus with T_m; this is essentially a more quantitative rephrasing of the mechanism discussed in the introduction. Other, possibly more accurate parameterizations of F_L exist [e.g., *Stone and Yao*, 1990]. However, (2) is appealingly simple and is adequate as a diagnostic tool in the identification of mechanisms responsible for the observed saturation of poleward energy flux.

[9] Figure 2a shows the F_L predicted by (2) under the simplest assumptions, constant V and constant source region latitude. Note that we make no attempt to predict the absolute value of F_L, which has been scaled arbitrarily for ease of comparison. The prediction is clearly far off the mark: latent heat flux grows exponentially with T_m everywhere. We can try to correct the estimate by taking values of V directly from the model (Figure 3a). The resulting prediction (Figure 2b) is closer to the model results, but still too sensitive to T_m at high temperatures.

[10] Accounting for the remaining discrepancy requires closer examination of changes in the structure of the model's general circulation. As shown in Figure 3b, increasing T_m results in poleward migration of the storm tracks. This has a moderating effect on F_L, both because the moisture source is now located over cooler waters, reducing $q_s(T_{\rm src})$, and because the storm track contracts zonally as it moves poleward, as reflected by the $\cos(\varphi)$ term in (1). Taking both factors into account leads to a prediction (Figure 2c) which captures the main qualitative features of the GCM results, in particular the saturation of F_L at high T_m.

[11] Finally, we need to account for the behavior of V shown in Figure 3a. Why should eddy kinetic energy first increase and then decrease as global mean temperature increases? Baroclinic instability theory suggests that the level of eddy activity is controlled by the horizontal and vertical temperature gradients of the background flow, usefully summarized by the Eady growth rate $\sigma_{BI} = 0.31\, f|\partial v/\partial z|N^{-1}$, where notation is standard [*Hoskins and Valdes*, 1990]. This quantity (Figure 3c) strongly decreases with increasing T_m. Since surface temperature is fixed, the decrease is due almost entirely to the static stability term. Decreasing σ_{BI} can account for the damping of eddy activity at high T_m, but is inconsistent with the increasing eddy activity seen at lower temperatures. *Lapeyre and Held* [2004], using a quasi-geostrophic model with fixed static stability, show that latent heat release energizes extratropical eddies, an effect that can be captured in a dry model using a reduced effective static stability. We speculate that this effect predominates at low T_m, while above $T_m = 15$°C it is overwhelmed by the increase in *actual* static stability.

4. Slab Ocean Runs

[12] To directly assess the role of F_L in controlling the meridional temperature gradient, we conduct a number of runs using NCAR's CCM3.6 at T21 resolution coupled to an aquaplanet slab ocean with prognostic surface temperature. Ocean albedo and fixed ocean energy transports are adjusted to obtain two base states using present-day $p\mathrm{CO}_2$ and annual-mean insolation: a warm, low-gradient state (case 1, $T_m = 30.7$°C, $\Delta T = 25.7$°C) and a cooler, higher-gradient state (case 2, $T_m = 20.2$°C, $\Delta T = 37.8$°C). We then compare with identical runs in which $p\mathrm{CO}_2$ is quadrupled. All these runs are permanently ice-free, and they all employ fixed, climatological cloud fraction and liquid water path distributions computed from a previous, variable-cloud run. Surface-albedo, cloud radiative forcing and ocean transport feedbacks have thus been deactivated in these runs, so changes in equator-to-pole temperature gradient caused by quadrupling $p\mathrm{CO}_2$ should be largely attributable to changes in poleward energy transport.

[13] Results are shown by the blue segments in Figure 1c. Quadrupling $p\mathrm{CO}_2$ leads to a ~2°C reduction of ΔT in case 2, while in case 1 ΔT increases slightly as the climate warms. This is consistent with poleward heat transport feedback: case 2 is in a regime where transport increases with T_m and thus reduces ΔT, while case 1 is in the saturated regime, where transport actually decreases slightly with T_m.

5. Summary and Conclusions

[14] We have studied the behavior of poleward energy transport in a GCM as a function of global mean temperature T_m and equator-to-pole temperature difference ΔT. For $T_m > 15$°C and $\Delta T < 30$°C, poleward heat transport becomes essentially independent of T_m. We attribute this behavior to two main dynamical causes: (1) the eddy kinetic

energy and hence diffusivity of the storm tracks decreases as T_m increases above 15°C, due to the overwhelming effect of increasing background static stability; (2) the storm tracks migrate poleward as T_m increases; the resulting decrease in moisture supply to the storm tracks and their zonal contraction diminishes their integrated poleward heat transport.

[15] Once climate has warmed sufficiently to melt back all ice and snow cover, with the consequent reduction in meridional temperature gradient through surface albedo feedback, there is thus little scope for further reduction in the gradient through increased poleward atmospheric heat transport in this GCM. One caveat to this conclusion is the aquaplanet configuration used here: varying land fraction and atmospheric stationary wave response due to changing paleogeography and sea level could in principle drive changes in poleward latent heat flux. A more fundamental question is the extent to which the mechanisms identified here actually operate in nature. This is a difficult question to answer given the current level of theoretical understanding of the processes involved. There is no general agreement, for instance, on the factors controlling the mean extratropical static stability. Available theories [*Held*, 1982; *Juckes*, 2000; *Schneider*, 2004] link static stability to meridional temperature gradients, but are silent as to the changes in static stability with global-mean temperature found here. It seems safe to surmise that moisture must be playing a leading part here, bringing into question the role of sub-grid-scale processes.

[16] Thus, resolving the low-gradient paradox may require a fundamental advance in our understanding of the atmospheric general circulation. It may still turn out that the saturation of latent heat flux found here is an artifact of current GCMs, while in nature (and in improved models) there is no such limit. Alternatively, the answer may lie in other mechanisms not included in the present generation of GCMs, such as high-latitude radiative warming by polar stratospheric clouds [*Sloan and Pollard*, 1998], or increased ocean heat transport driven by tropical cyclone-induced mixing [*Emanuel*, 2002].

[17] **Acknowledgments.** Thanks to Matt Huber for helpful comments. We gratefully acknowledge use of "Jazz," a 350-node computing cluster operated by the Mathematics and Computer Science Division at Argonne National Laboratory as part of its Laboratory Computing Resource Center. Work supported by NSF ATM-0121028.

References

Barron, E. J. (1987), Eocene equator-to-pole surface ocean temperature: A significant climate problem?, *Paleoceanography*, *2*, 729–739.

Crowley, T. J., and J. C. Zachos (2000), Comparison of zonal temperature profiles for past warm periods, in *Warm Climates in Earth History*, edited by B. Huber, K. G. MacLeod, and S. C. Wing, pp. 50–76, Cambridge Univ. Press, New York.

Dong, B., and P. J. Valdes (2000), Climates of the Last Glacial Maximum: Influence of model horizontal resolution, *J. Clim.*, *13*, 1554–1573.

Emanuel, K. (2002), A simple model for multiple climate regimes, *J. Geophys. Res.*, *107*(D9), 4077, doi:10.1029/2001JD001002.

Greenwood, D. R., and S. L. Wing (1995), Eocene continental climates and latitudinal temperature gradients, *Geology*, *23*, 1044–1048.

Hay, W. W., R. M. DeConto, and C. N. Wold (1997), Climate: Is the past key to the future?, *Geol. Rundsch.*, *86*, 471–491.

Held, I. M. (1982), On the height of the tropopause and the static stability of the troposphere, *J. Atmos. Sci.*, *32*, 412–417.

Hoskins, B. J., and P. J. Valdes (1990), On the existence of storm-tracks, *J. Atmos. Sci.*, *47*, 1854–1864.

Huber, M., and L. Sloan (1999), Warm climate transitions: A general circulation modeling study of the Late Paleocene Thermal Maximum (~56 Ma), *J. Geophys. Res.*, *104*, 16,633–16,655.

Huber, M., and L. Sloan (2001), Heat transport, deep waters and thermal gradients: Coupled climate simulation of an Eocene greenhouse climate, *Geophys. Res. Lett.*, *28*, 3481–3484.

Jacob, R. (1997), Low frequency variability in a simulated atmosphere ocean system, Ph.D. thesis, Univ. of Wis.-Madison, Madison.

Juckes, M. N. (2000), The static stability of the midlatitude troposphere: The relevance of moisture, *J. Atmos. Sci.*, *57*, 3050–3057.

Kiehl, J. T., J. J. Hack, G. B. Bonan, B. A. Boville, B. P. Brieglieb, D. L. Willliamson, and P. J. Rasch (1996), Description of the NCAR Community Climate Model (CCM3), *Tech. Rep. TN-420*, Natl. Cent. for Atmos. Res., Boulder, Colo.

Lapeyre, G., and I. M. Held (2004), The role of moisture in the dynamics and energetics of turbulent baroclinic eddies, *J. Atmos. Sci.*, *61*, 1693–1710.

Manabe, S., and R. T. Wetherald (1980), On the distribution of climate change resulting from an increase in the CO_2 content of the atmosphere, *J. Atmos. Sci.*, *37*, 99–118.

Norris, R. D., K. L. Bice, E. A. Magno, and P. A. Wilson (2002), Jiggling the tropical thermostat in the Cretaceous hothouse, *Geology*, *30*, 299–302.

Pierrehumbert, R. T. (2002), The hydrological cycle in deep-time climate problems, *Nature*, *419*, 191–198.

Rind, D. (1998), Latitudinal temperature gradients and climate change, *J. Geophys. Res.*, *103*, 5943–5971.

Schmidt, G. A., and L. A. Mysak (1996), Can increased poleward oceanic heat flux explain the warm Cretaceous climate?, *Paleoceanography*, *11*, 579–593.

Schneider, T. (2004), The tropopause and the thermal stratification in the extratropics of a dry atmosphere, *J. Atmos. Sci.*, *61*, 1317–1340.

Sloan, L. C., and D. Pollard (1998), Polar stratospheric clouds: A high latitude warming mechanism in an ancient greenhouse world, *Geophys. Res. Lett.*, *25*, 3517–3520.

Stone, P. H., and M. S. Yao (1990), Development of a two-dimensional zonally averaged statistical-dynamical model. Part III: The parameterization of the eddy fluxes of heat and moisture, *J. Clim.*, *3*, 726–740.

R. Caballero, Department of the Geophysical Sciences, University of Chicago, 5734 South Ellis Avenue, Chicago, IL 60637, USA. (rca@geosci.uchicago.edu)

P. L. Langen, Department of Geophysics, University of Copenhagen, Juliane Maries Vej 30, DK-2100, Copenhagen Ø, Denmark. (plangen@gfy.ku.dk)